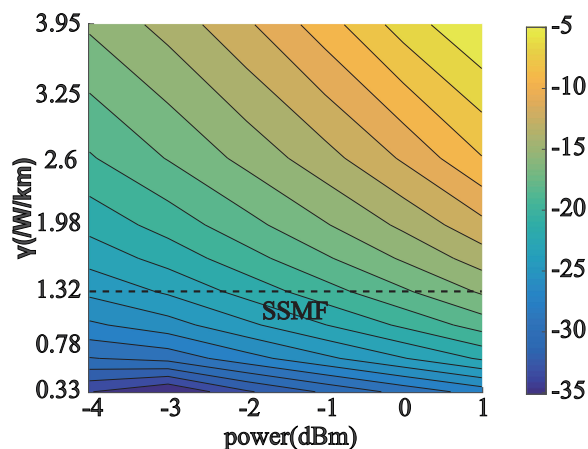


A Joint OSNR and Nonlinear Distortions Estimation Method for Optical Fiber Transmission System

Volume 10, Number 5, September 2018

Yating Xiang
Ming Tang, *Senior Member, IEEE*
Qiong Wu
Huibin Zhou
Bo Yong
Songnian Fu
Deming Liu



DOI: 10.1109/JPHOT.2018.2873778

1943-0655 © 2018 IEEE

A Joint OSNR and Nonlinear Distortions Estimation Method for Optical Fiber Transmission System

Yating Xiang¹,¹ Ming Tang¹,¹ Senior Member, IEEE, Qiong Wu,¹
Huibin Zhou,¹ Bo Yong,² Songnian Fu¹,¹ and Deming Liu¹

¹Wuhan National Laboratory for Optoelectronics and Next Generation Internet Access
National Engineering Laboratory, School of Optical and Electronic Information, Huazhong
University of Science and Technology, Wuhan 430074, China

²Fiberhome Telecommunication Technologies Co., Ltd, Wuhan 430074, China

DOI:10.1109/JPHOT.2018.2873778

1943-0655 © 2018 IEEE. Translations and content mining are permitted for academic research only.

Personal use is also permitted, but republication/redistribution requires IEEE permission.

See http://www.ieee.org/publications_standards/publications/rights/index.html for more information.

Manuscript received August 31, 2018; accepted September 28, 2018. Date of publication October 4, 2018; date of current version October 17, 2018. This work was supported in part by the National Natural Science Foundation of China under Grants 61331010 and 61722108; and in part by the Fundamental Research Funds for the Central Universities' under Grant HUST: 2018KFYXKJC023. Corresponding author: M. Tang (e-mail: tangming@mail.hust.edu.cn.)

Abstract: In this paper, we propose and demonstrate a joint optical signal-to-noise ratio (OSNR) and a nonlinear distortions estimation method. The OSNR is calculated by considering either the link parameters or the correlation operations of the training symbols. The nonlinear distortions estimation in this calculation comes from different nonlinear sensitivities of these two methods. The indicator of NL penalty is defined as the ratio of nonlinear distortion power to the signal power. As the estimation method, based on link parameters, has low computational complexity, and the training symbol used for the OSNR estimation is inherently indispensable for frame synchronization, this nonlinear distortion estimation method introduces a few complexities and no extra overhead. Experimental results obtained by using a 200 Gb/s 16 QAM DWDM system establish the accuracy of the proposed OSNR estimations method, with errors less than 1 dB. The nonlinear distortions were also measured under different simulation conditions, using a coherent optical OFDM system, and the results are in accordance with the expectations.

Index Terms: Optical signal-to-noise ratio (OSNR), nonlinear distortion, training symbol (TS).

1. Introduction

In Recent years, following the explosive growth in bandwidth demand, high-order modulation formats and dense wavelength division multiplexing (DWDM) have been increasingly applied to improve spectrum efficiency and expand communication capacity. Concurrently, the next generation reconfigurable optical network has started looking for flexible grid size, adaptive modulation formats and transmission rate, according to the bandwidth requirements and channel conditions. Whether it is traditional static optical network or future dynamic optical network, the basic requirements for an efficient and reliable optical network are performance monitoring, fault location and damage repair.

For decades, optical signal-to-noise ratio (OSNR) has been a key parameter for optical performance monitoring (OPM). The transmission systems can function well only within a proper range of OSNRs. Many methods were proposed for in-band OSNR estimation, such as polarization nulling

[1], narrow bandwidth filters [2], optical delay interferometer [3], delay-tap sampling [4] and training symbols [5]. However, higher launch power and denser grid allocation introduce considerable nonlinear (NL) distortions into the communication system, such as self-phase modulation (SPM), cross-phase modulation (XPM), and four-wave mixing (FWM). The accuracy of some of the above mentioned OSNR estimation methods are reduced by the NL distortions. Therefore, many NL insensitive OSNR estimation methods have been reported. The OSNR can be estimated by adding LFM signal pilots [6], adding differential pilots [7], [8], using statistical moments [9], or utilizing the correlation function [10]. High accuracy and large nonlinear tolerance are achieved by these methods. However, some of these methods reduce the spectrum efficiency by adding pilots, or improve the complexity of DSP. We intend to use a straightforward and more cost-effective method, based on transmission link parameters, to measure the NL insensitive OSNR.

Since the NL distortions damage the signal quality to such an extent that the original signals cannot be recovered even with a high OSNR, the signal quality can no longer be judged by OSNR performance alone. Therefore, to calculate the performance limits, it is mandatory to consider NL distortions, together with the OSNR, as an indicator.

Previously, a series of NL estimation and compensation methods were reported. Digital back propagation technique was investigated in [11] to mitigate inter-channel nonlinearity. In [12], a time domain approach, utilizing perturbative model, was proposed in uncompensated links propagation. In [13] and [14], equalizers, based on fiber third-order Volterra kernels, were introduced in frequency domain. These models play the main role of nonlinear estimation and compensation, but, in doing so, they introduce high complexity. This necessitates a cost-effective method, without complicated digital signal processing (DSP), for the OPM, before establishing and compensating for the nonlinear model. For instance, when the modulation format alters from Quadrature Phase Shift Keying (QPSK) to 16 quadrature amplitude modulation (QAM) or 64 QAM, timely NL distortions estimation will be required for power budget adjustment. NL distortions estimation is also essential, especially, in a reconfigurable optical add-drop multiplexers (ROADM) enabled network, because NL distortions constrain the designing of the number and channel spacing of additional channels.

In this paper, the authors propose a joint in-band OSNR and NL monitoring method, supported by transmission link parameters and training symbols. On the one hand, a NL distortion-insensitive OSNR is estimated, using link parameters, such as EDFA gains, noise figures and optical signal powers, in the cascaded erbium-doped optical fiber amplifiers (EDFAs) fiber communication system. As NL distortions only affect the signal quality without impacting the signal power, this method is insensitive to NL distortions. On the other hand, the OSNR monitoring method, based on training symbols, derives OSNR from a priorly calibrated relationship between OSNR and electrical signal-to-noise ratio (ESNR), and the ESNR from a correlation operation of the training symbols [5]. For this method, NL distortions can be viewed as the additional noise, based on the GN model [15], which will influence OSNR estimation performance. Thus, it is reasonable to conclude that the difference between the OSNRs estimated by these two methods reflects the NL distortions of the same system. As monitoring of link parameters is, by default, a part of network management system, using training symbols is inevitable for calculating ESNR for frame synchronization, and hence the joint estimation method, which is being proposed here, does not introduce any extra overhead. Validation of the efficacy of the proposed estimation method is demonstrated through simulations, using MATLAB and VPI Transmission Maker 9.1.

The remainder of this paper is organized as follows: Section II presents the theory behind the OSNR monitoring method, based on link analysis, and demonstrates it through a 200 Gb/s 16QAM experiment; Section III presents the proposed NL estimation method and validates its reliability through simulations; finally, the conclusions drawn from this study are presented.

2. Principle of OSNR Monitoring

In the OSNR estimation method, supported by transmission link parameters, OSNR penalty results from the ASE noise that accumulates in the cascaded EDFAs. The ASE noise power and the noise

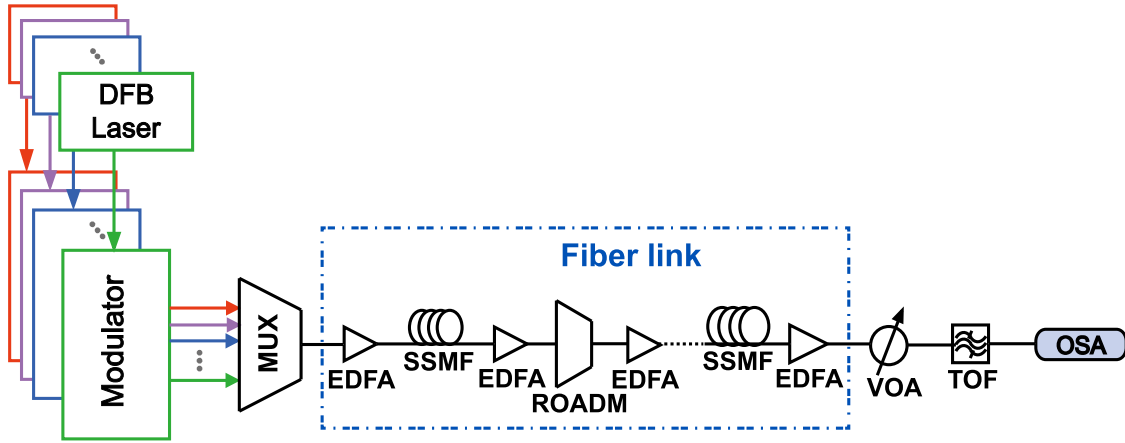


Fig. 1. Experimental setup. DFB laser: Distributed feedback laser; MUX: Multiplexer; EDFA: Er3+ doped fiber amplifier; SSMF: Standard single mode fiber; ROADM: Reconfigurable optical add-drop multiplexer; VOA: Variable optical attenuator; TOF: Tunable optical filter; OSA: Optical spectrum analyzer.

figure (NF) that measure degradation of SNR in an EDFA are expressed as follows:

$$P_{ASE} = 2n_{sp}(G - 1)h\nu B_0 \quad (1)$$

$$F = \frac{SNR_{in}}{SNR_{out}} = \frac{P_{ASE}}{h\nu B_0 G} + \frac{1}{G} \quad (2)$$

where P_{ASE} stands for ASE noise power, n_{sp} for spontaneous emission factor, G for EDFA gain, h for the Planck constant, which equals to 6.625×10^{-34} Ws², ν for signal frequency, B_0 for optical bandwidth in 1.55 μ m windows (usually 0.1 nm) [16], and F for NF, denoting the ratio of input and output SNRs of an EDFA. Thus, ASE noise is calculated using (3). OSNR is the ratio of signal power P_{sig} and total noise power P_{ASE}^{tot} , which is the sum of P_{ASE} in all EDFAs (4).

$$P_{ASE} = \left(F - \frac{1}{G}\right) h\nu B_0 G \quad (3)$$

$$OSNR = \frac{P_{sig}}{P_{ASE}^{tot}} = \frac{P_{in} \prod_{m=2}^{N-1} \Delta_m G_N}{\sum_{n=1}^{N-1} P_{ASE}^i L_i \prod_{m=i+1}^{N-1} \Delta_m G_N + P_{ASE}^N} \quad (4)$$

P_{in} is the EDFA's input signal power, and Δ_m is the product of gain in m th EDFA and loss in m th fiber, which can be further simplified as follows:

$$\frac{1}{OSNR_{N_2}} = \frac{1}{OSNR_{N_1}} + \frac{h\nu B_0}{P_{inN_1}} F_{N_1N_2} \quad (5)$$

$$F_{N_1N_2} = \sum_{N_1+1}^{N_2} \frac{F_j - L_{j-1}}{\prod_{m=1}^{j-1} \Delta_m} \quad (6)$$

where $F_{N_1N_2}$ is an equivalent NF of the link between two arbitrary amplifiers EDFA_{N₁} and EDFA_{N₂}, indicating that the OSNR penalty can be linearly added to the inverse of OSNR. As the link condition changes from time to time, the only thing that needs to be watched is the current $F_{N_1N_2}$ value.

The accuracy of this estimation method was verified through experiments on 150 Gb/s 8 QAM and 200 Gb/s 16 QAM DWDM transmission system, with 1400-km standard single mode fiber (SSMF). The experimental setup is shown in Fig. 1. The transmission link consists of 14 spans of 100 km SSMF and 3 ROADMs, which are linked by EDFAs to compensate for their losses. The loss of fiber and connector of each span is variable around 25 dB, and each ROADM attenuates the power by about 7 dB. Gains of EDFAs range from 14 dB to 25 dB on demand, because each EDFA imposes a

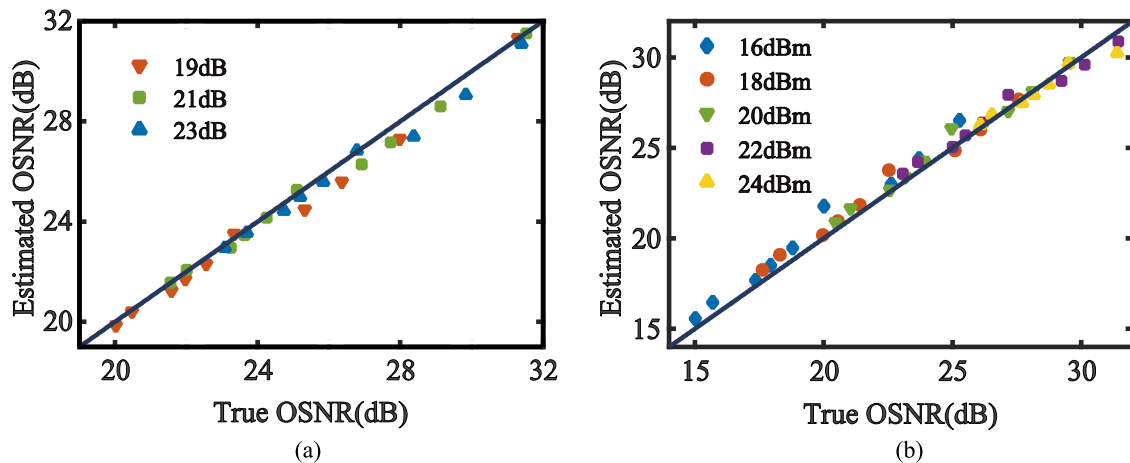


Fig. 2. Relationship of Estimated OSNR vs. True OSNR. (a) With different gains of the first EDFA. (b) With different output powers of the first EDFA.

gain tilt of about -1 dB among the 96 channels, due to uneven Erbium-doped fiber gain spectrum. Thus, pre-emphasis of 0.625 dB/THz was implemented by the ROADMs on every 3 EDFAs to flatten the powers of all channels. EDFAs' noise figures range from 3 dB to 6 dB, denoting the OSNR penalty of ASE noise. Among the 96 channels, which range from 191.30 – 196.05 THz with 50 GHz channel spacing, only 12 channels contain signals while the others are filled with Gaussian white noise for simplicity.

In the experiments, the gains of the first EDFA were altered over a range of 19 – 23 dB and the output OSNR of each EDFA estimated to cover an OSNR range of 15 – 30 dB. Then, the estimated OSNRs of channels 1, 3, 94, and 96, obtained from the formulas given above, were compared with the measured OSNRs by optical spectrum analyzer (OSA), using integral method. This estimation method was proved to be highly accurate, with estimation errors of less than 1 dB, regardless of the gains or output powers. As all the four channels performed similarly, the performance of only channel 94 is illustrated here (see Fig 2(a)). Then, the gains of EDFA were fixed and its output powers swept from 16 – 24 dBm. The above process was repeated, and the results were found to be the same, as shown in Fig. 2(b).

In this experiment, the input power of each channel can be set and confirmed in the network management system. The noise figure of each EDFA among the EDFA's gain spectrum, under different input powers, is measured and uploaded to the network management system as well. Thus, it is convenient to directly read the system parameters of an aimed channel. As the centralized software defined optical network technology develops, system parameters tend to be more transparent and available. Thus, this method is easier, more cost-effective and independent of algorithm and device, compared with DSP based methods.

As the NL distortions governed by SPM and XPM are elastic, in the sense that no energy is exchanged between the electromagnetic field and the dielectric medium, they lead to spectral and temporal changes in the optical wave without changing its energy [17]. And, as this method is concerned only with the powers of signals and ASE noises, it can be inferred to be insensitive to NL distortions. To confirm this hypothesis, a series of simulations were conducted with MATLAB and VPI Transmission Maker 9.1. In a 10×100 km coherent optical transmission system (the same CO-OFDM system was used thereafter and will be described in more detail below), the fibers' nonlinear parameter γ was set to vary from 0 to 3.95 W/km. For each setting, the fiber input power was swept from -10 to $+10$ dBm. Under the same input power, the simulation results show no obvious difference among the OSNRs, despite variations in NL parameters; besides, for different input powers, all the estimation results are in accordance with the expectations presented in Fig. 3. It means that this method is nonlinearity insensitive. Since the theoretical model of this OSNR estimation method is based merely on link parameters, it can be inferred that the method is

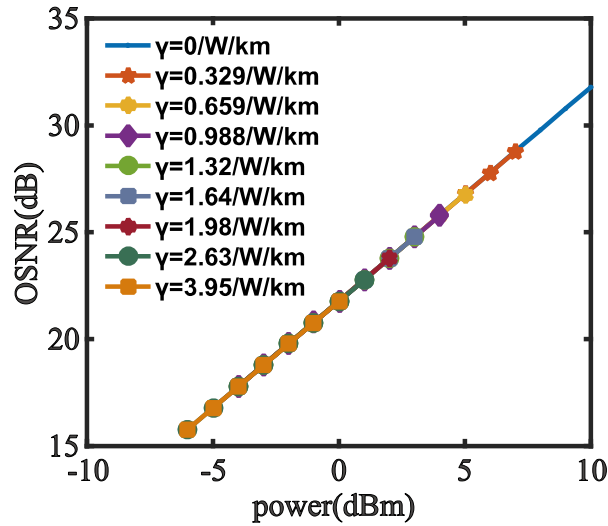


Fig. 3. Relationship of OSNR vs. Power under different nonlinear parameters (γ).

adaptable whatever the modulation formats or multiplexing technology are. Simulation results prove it to be accurate and applicable in multi-carrier, as well as single carrier systems.

Based on the principles of OSNR estimation and NL distortions, and the simulation results, a modified OSNR model is proposed here, as shown below by (7). Despite varying NL distortions, the total signal power P_{sig}^{tot} remains unchanged, which includes two parts, namely, the equivalent power of NL distortions P_{NL} denoting the signal degradation due to nonlinearity, and the equivalent signal power P_{sig} , which is not affected by NL. Higher NL distortions merely raise the proportion of P_{NL} , but they do not change either the total power P_{sig}^{tot} or the estimated $OSNR^I$. In a way, $OSNR^I$'s incapability of representing NL influences, necessitates evaluation criteria for NL distortions.

$$OSNR^I = \frac{P_{sig}^{tot}}{P_{ASE}} = \frac{P_{sig} + P_{NL}}{P_{ASE}} \quad (7)$$

3. Principle of NL Monitoring

The dependence of refractive index on power is responsible for the Kerr-effect [17], which results in nonlinear distortions of optical fiber transmission. The Kerr effect is determined mainly by the nonlinear parameter γ , which bears a standard relation with nonlinear-index coefficient n_2 , as shown in (8). The nonlinear phase shift is then expressed by (9):

$$\gamma = 2\pi n_2 / (\lambda A_{eff}) \quad (8)$$

$$\phi_{NL} = \gamma PL_{eff} \quad (9)$$

where P is the optical power, A_{eff} is the effective mode area, which, by default, is $80 \times 10^{-12} \text{ m}^2$ in SSMF, and L_{eff} is the effective length of the fiber, which depends only on fiber attenuation.

Derivation of NL distortions by the proposed method involves two steps. First, the OSNR, which is insensitive to NL distortions, is calculated by the transmission link parameters, as explained above. Then, utilizing the correlation operation of training symbols, OSNR with ASE noise and the NL distortions involved, are acquired. The NL distortion can be acquired by simple computation.

In OSNR monitoring method based on training symbols, for a coherent optical OFDM system, every subcarrier contains several frames for both X and Y polarizations. For each frame, a series of training symbols TS1 and TS2 are generated ahead of data. The frame structure of the training symbols is depicted in Fig. 4. After transmission and coherent reception, TS1 are used for symbol synchronization in both polarizations. Through fast Fourier transform (FFT) operation, the received

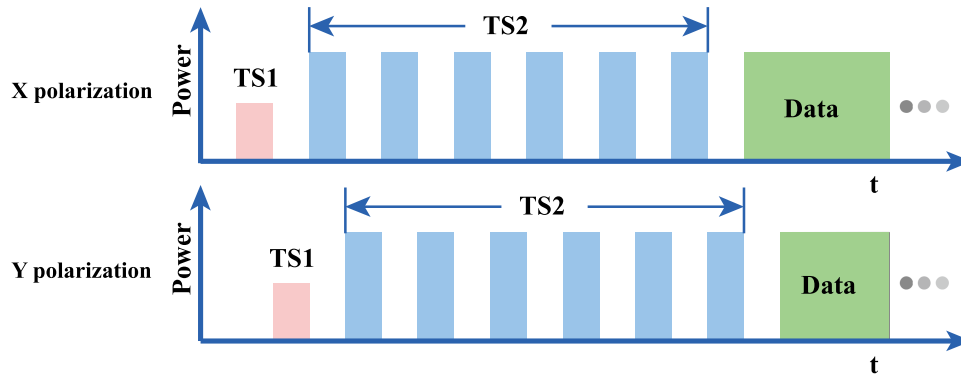


Fig. 4. Frame structure of training symbols.

signals are transferred to the frequency domain. Then, the remaining training symbols TS2 are utilized for polarization demultiplexing and channel estimation. From the received data, only TS1 need to be recovered for ESNR calculation, and this greatly reduces computational complexity. The received TS1 of the k -th subcarrier in X polarization can be expressed as (10):

$$c_X(k) = H(k) \cdot s_X(k) + n_X(k) \quad (10)$$

where $H(k)$ denotes the channel's transmission function, $c_X(k)$ and $s_X(k)$ the received and original TS1, and $n_X(k)$ the noise in the channel. The noise is supposed to be normally distributed and not correlated with the signal. Autocorrelation of $c_X(k)$ and cross-correlation between $c_X(k)$ and $s_X(k)$, to obtain the ESNR, are conducted, using the following equations:

$$R_{auto} = |H|^2 \cdot R_s(0) + R_n(0) \quad (11)$$

$$R_{xcorr} = H \cdot R_s(0) \quad (12)$$

$$ESNR = \frac{P_s}{P_n/|H|^2} = \frac{|R_{xcorr}|^2}{R_{auto} \cdot R_s(0) - |R_{xcorr}|^2} \quad (13)$$

where $R_s(0)$ and $R_n(0)$ represent, respectively, autocorrelation of signal $c_X(k)$ and noise $n_X(k)$ with zero delay. According to [18], the inverse of OSNR obeys a linear relationship with the inverse of ESNR, as shown below:

$$\frac{1}{ESNR} = A \frac{1}{OSNR} + B \quad (14)$$

In this formula, A is a proportional constant between ESNR and OSNR, and B a constant, relevant to the transmitters' and receivers' background phase noises [18]. Both A and B can be calibrated by measuring ESNRs against a series of known OSNRs and performing a linear fit between $1/ESNR$ and $1/OSNR$ [18]. Based on this formula, OSNR can be derived from ESNR.

In this DSP-based OSNR estimation method, the NL distortions cannot be ignored, because the GN model considers P_{NL} as additional Gaussian noise that can be directly added to the signals. After polarization demultiplexing and channel estimation, fiber's linear effects such as different kinds of dispersions can be eliminated, however, ASE noise and NL distortion remain. Thus, ESNR can act as an accurate indicator of them, and it is the same with OSNR estimated with this method. This OSNR is expressed as $OSNR^{II}$ to distinguish it from $OSNR^I$ (15), as shown below:

$$OSNR^{II} = \frac{P_{sig}}{P_{ASE} + P_{NL}} \quad (15)$$

The traditional OSNR concerns mainly the NL insensitive OSNR monitoring, such as $OSNR^I$. However, this $OSNR^{II}$ is inherently sensitive to NL distortion as ESNR does. It might be better to

TABLE 1
Comparison of the Two OSNR Methods

Method	I	II
Principle	Link parameters	Digital signal processing
Parameters	P_{in}, G, F, L .	Training symbols
Operations	Equivalent NF calculation of the cascaded EDFA link	ESNR estimation Calibration from the estimated ESNR
NL embodiment	Signal distortion	Noise
Expression	$OSNR^I = \frac{P_{sig} + P_{NL}}{P_{ASE}}$	$OSNR^{II} = \frac{P_{sig}}{P_{ASE} + P_{NL}}$

describe it as “augmented OSNR”, which bring into the impact from fiber nonlinearity. Now, two different OSNR models, $OSNR^I$ and $OSNR^{II}$, are available, which are based on different OSNR estimation principles: link parameters and digital signal processing. Table 1 shows the comparison between these two models.

The relationship between these two models, $OSNR^I$ with $OSNR^{II}$, can be obtained by using three variables (P_{sig} , P_{ASE} and P_{NL}) and simple conversion (see Eq (16)). It emerges that the approximation can be made only if $OSNR^I$ is far greater than 1.

$$\frac{P_{NL}}{P_{sig}} = \frac{OSNR^I - OSNR^{II}}{OSNR^{II}(1 + OSNR^I)} \approx \frac{1}{OSNR^{II}} - \frac{1}{OSNR^I} \quad (16)$$

The ratio of P_{NL} and P_{sig} , named as NL penalty, may serve as a performance metric for NL distortions, the same way as OSNR does. As this ratio shares the same scale and denotes the relationship between signals and distortions as OSNR does, the proposed NL penalty can be naturally subsumed into the current OPM evaluation standard.

We just used simulation systems to investigate the second OSNR estimation method and NL monitoring based on two reasons. One is that it is not feasible to change the DSP scheme of the commercial transmission system setup we used in the experiment of the first OSNR estimation. Another is that only in the simulation can we easily change the nonlinearity by setting different input power and fiber’s nonlinear parameters. The simulation’s setup is shown in Fig. 5. At the transmitter, the offline DSP produces and encodes two independent data sequences, which were sampled with 32 GSa/s rate in X polarization and Y polarization, generated from AWG and modulated with IQ modulators. A pair of polarization beam splitter/combiner was used to separate the two optical carriers and join the two tributaries. The signals were then transmitted through a fiber link, having 10 spans of 100 km SSMFs, whose losses were compensated with EDFAs. The output power was adjustable with a variable optical attenuator (VOA). At the receiver, a tunable optical filter was used to extract the required bandwidth and remove the out-band noise, and then the signals transmitted through an electrical amplifier. Afterward, the signals go through two PBSs and a pair of 90° hybrids, and then detected with four balanced photodiodes. A chain of DSP operations was conducted, which included frequency offset compensation, frame synchronization, polarization demultiplex, ESNR calculation, OSNR calibration and NL estimation.

First, γ was set as 0 to ensure that that no NL distortion is added, the degradation of ESNR only results from the ASE noise. In order to obtain A and B in (14), a linear fitting between a series of 1/OSNRs and 1/ESNRs was performed. The 1/OSNRs are of different launch powers, measured by signal analyzers in VPI, and the 1/ESNRs are computed with (11)–(13) in Matlab. This calibration procedure is the same as that described in [5], except for the difference in A and B due to different background phase noises of two systems. For simplicity, we just give the result that, in the X polarization, $1/OSNR = 0.4734 \times 1/ESNR - 0.0006595$, while in the Y polarization, $1/OSNR = 0.5672 \times 1/ESNR - 0.0007916$.

According to (9), power and NL are the two important parameters that determine the strength of the nonlinear distortions in the fiber. To check this, the launch powers of laser (−6 to 10 dBm) and

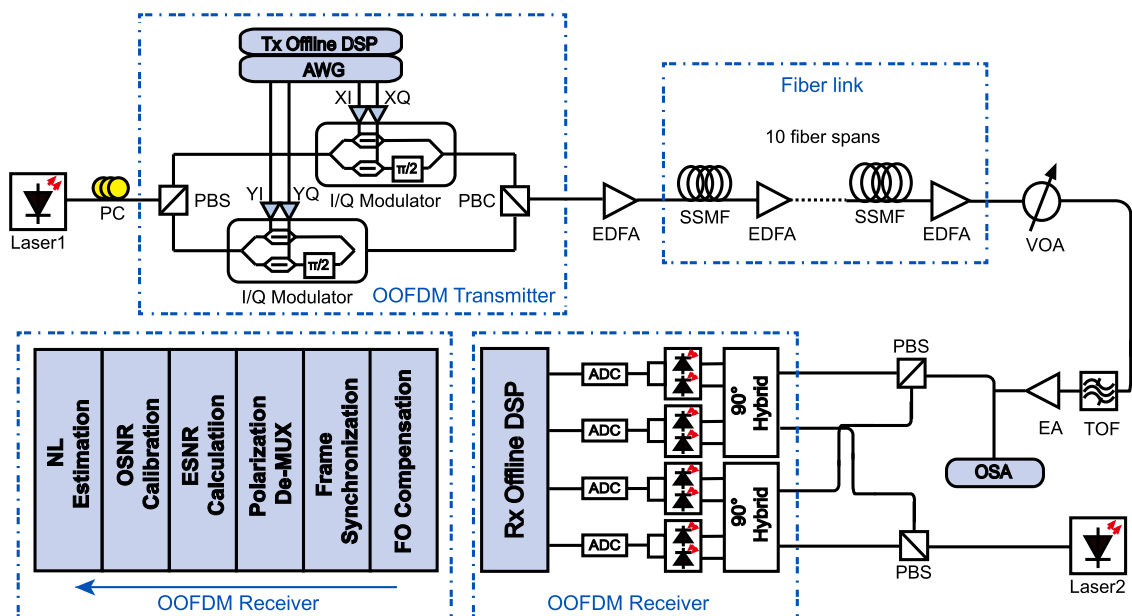


Fig. 5. Simulation setup. AWG: Arbitrary waveform generator; PC: Polarization controller; PBS/C: Polarization beam splitter/combiner; EDFA: Er3+ doped fiber amplifier; VOA: Variable optical attenuator; TOF: Tunable optical filter; OSA: Optical spectrum analyzer; ADC: Analog-to-digital converter; FO: Frequency offset.

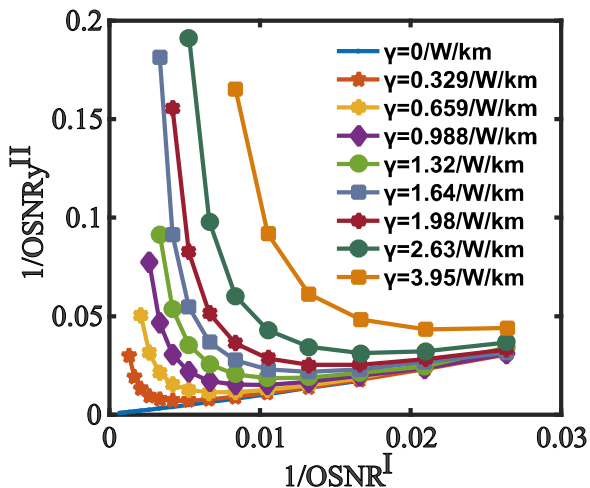


Fig. 6. Calibrated $1/OSNR^{II}$ with ESNR vs. $1/OSNR^I$ relationship, acquired from link parameters under different NL parameters.

the nonlinear parameter γ of fibers (0 to 3.95/W/km) were varied, the ESNRs recorded, and the corresponding $OSNR^{II}$ s calculated to check the outcome.

It was found that, except for the slight influence due to polarization-dependent loss, there was hardly any difference between the $OSNR^{II}$ s of the two polarization tributaries. Figure 6 shows the calibrated $1/OSNR^{II}$ in Y polarization tributaries versus $1/OSNR^I$ relationship, obtained by link analysis (both in a linear unit). The figure shows that $1/OSNR^{II}$ sustains the same pace with $1/OSNR^I$, when γ was set to 0 without any nonlinear distortions. When the fiber input powers were small, which means that both the OSNRs and NL distortions were small, as shown in the right side of the figure, the lines with all degrees of NL parameters tended to get close to the asymptote, with

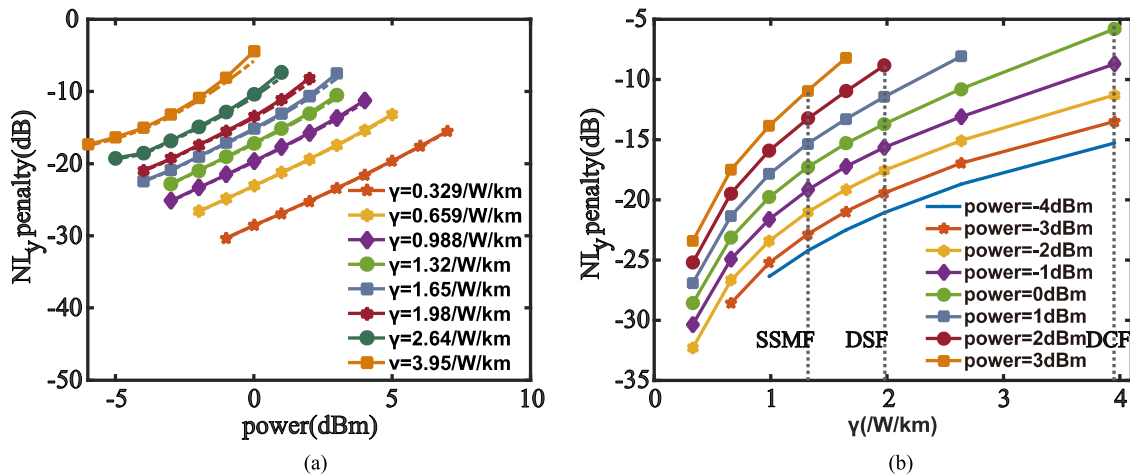


Fig. 7. (a) Relationship of NL penalty vs. input power, under different NL parameters. (b) Relationship of NL penalty vs. NL parameter, under different powers.

the slope equaling 1, where no NL distortions existed. As the input powers increased, as shown in the left side of the figure, NL distortions rose rapidly, and $1/OSNR^{II}$ was deviated from $1/OSNR^I$, especially when the NL parameters was large.

Taking advantage of (16), the relationship of NL penalty of signals in Y polarization (in dB unit) versus power, under different NL parameters, is shown in Fig. 7. The green line, which denotes that γ is 1.32/W/km, stands for the SSMF that is universally utilized in optical communication systems. When the input power was high, NL penalty was linearly dependent on power. With lower input powers, the OSNRs became subsequently lower, leading to increase in approximation deviation in (16), and making the lines with large γ appear concave, as the solid lines show. In contrast to this, the dashed lines show the precise NL penalty without approximation. It is found that, without approximation, the concave lines became flatter, though not straight. The authors consider that further exploration is needed to find an explanation for this.

As already demonstrated above, the noise includes two parts, the ASE noise and the NL distortion, the former having no relation to the signal power, and the latter being proportional to the signal power. As the power increases, NL distortion starts dominating the ASE noise, and thus one can get optimal signal power with the lowest total noise. The optimal signal power decreased as the NL parameter became larger. As NL distortion is derived by subtracting the ASE noise from the total noise, the estimation result is more accurate in the NL distortion-dominant region. On the contrary, when the ASE noise is dominant, the performance difference in its estimation between the two methods is comparable to the NL distortion, and hence it becomes difficult to extract the exact amount of nonlinearity. In general, this NL estimation method is better used for SSMF or fibers with higher NL parameter.

The measured value of n_2 for silica fiber varies over a wide range, from 2.20 to 3.95×10^{-20} m²/W, depending on the fiber type and the technique used [19]. Also, effective mode area, which again depends on the fiber used, influences the NL parameter likewise. Therefore, the relationship of NL penalty versus NL parameter, under different input powers, is shown in Fig. 7. For a better understanding, the fiber types are marked as SSMF, dispersion-shifted fiber (DSF), and dispersion-compensating fiber (DCF) with dotted lines. Their NL penalty versus power relationships are in accordance with the predicted trends.

Overall, it can be concluded that NL penalty is positively related to power, as also to NL parameter, as can be seen from Fig. 7.

For a more intuitive and quantified cognition, using a pair of certain input power and nonlinear parameter, a contour map was drawn (see Fig. 8) to show how the magnitude of NL distortions changes with contributions from both power and nonlinear parameter. This is illustrated by marking

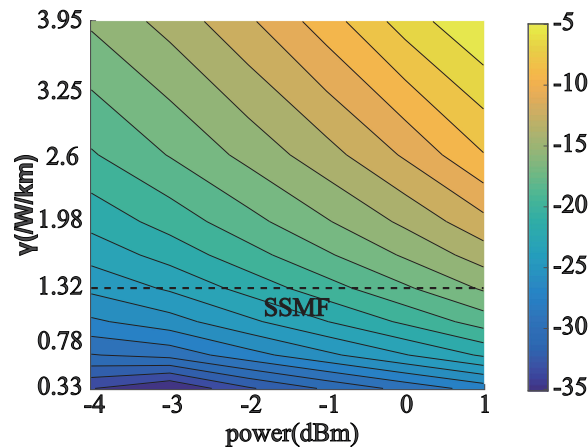


Fig. 8. Contour map of NL penalty.

a series of contours with uniform spacing and using the colorbar to represent NL penalty. Increase in both power and NL parameter led to increase NL penalty. A dashed line was drawn where the value of γ is 1.32/W/km, which stands for SSMF. When the launch power was rather low, the NL distortion became susceptible to ASE noise; on the other hand, when it was high, the NL distortion became so large that the signals deteriorated too severely to be recovered. However, it is noticed that NL penalty may not be the minimum when the input power is the lowest, because ASE noises perform overwhelmingly, compared with NL distortions, under low input power and small NL parameter conditions.

4. Conclusion

In this paper, the authors have proposed a joint OSNR and nonlinear distortions estimation method. The OSNR is calculated by using either the link parameters or the correlation operations in Rx DSP, both of which are cost-effective. The accuracy of the link parameters-based OSNR method was verified through experiments on a 200 Gb/s 16 QAM DWDM system, and the DSP-based method, through simulations. According to the authors' analysis, these two methods follow different OSNR calculation models and, therefore, have different NL sensitivities. Therefore, the influences of NL distortions, due to difference between the two OSNR calculation models, were extracted and the ratio of nonlinear distortion power to the signal power defined as the NL penalty to indicate solely the nonlinearity induced impairment. The results of simulation under different conditions, using a coherent optical OFDM system, establish that the proposed method is effective for estimating nonlinear distortions. From the estimated NL distortion, one can get a more comprehensive assessment of the signals' quality, besides OSNR. Also, the proposed method can be used to estimate the optimal power budget required for flexible grid ROADMs enabled networks.

References

- [1] J. H. Lee, H. Y. Choi, S. K. Shin, and Y. C. Chung, "A review of the polarization-nulling technique for monitoring optical-signal-to-noise ratio in dynamic WDM networks," *IEEE J. Lightw. Technol.*, vol. 24, no. 11, pp. 4162–4171, Nov. 2006.
- [2] Q. Li, K. Padmaraju, D. F. Logan, J. J. Ackert, A. P. Knights, and K. Bergman, "A fully-integrated in-band OSNR monitor using a wavelength-tunable Silicon microring resonator and photodiode," in *Proc. Int. Conf. Opt. Fiber Commun.*, 2014, pp. 1–3.
- [3] Z. Huang *et al.*, "Guideline of choosing optical delay time to optimize the performance of an interferometry-based in-band OSNR monitor," *Opt. Lett.*, vol. 41, no. 18, pp. 4178–4181, Sep. 2016.
- [4] Y. Yu, B. Zhang, and C. Yu, "Optical signal to noise ratio monitoring using single channel sampling technique," *Opt. Lett.*, vol. 22, no. 6, pp. 6874–6880, Mar. 2014.

- [5] Q. Wu *et al.*, "Training symbol assisted in-band OSNR monitoring technique for PDM-CO-OFDM system," *IEEE J. Lightw. Technol.*, vol. 35, no. 9, pp. 1551–1556, May 2017.
- [6] W. Wang, A. Yang, P. Guo, Y. Lu, and Y. Qiao, "Joint OSNR and interchannel nonlinearity estimation method based on fractional Fourier transform," *IEEE J. Lightw. Technol.*, vol. 35, no. 20, pp. 4497–4506, Oct. 2017.
- [7] L. Dou *et al.*, "Differential pilots aided in-band OSNR monitor with large nonlinear tolerance," in *Proc. Int. Conf. Opt. Fiber Commun.*, 2015, Paper W4D.3.
- [8] L. Dou *et al.*, "An accurate nonlinear noise insensitive OSNR monitor," in *Proc. Int. Conf. Opt. Fiber Commun.*, 2016, Paper W3A.5.
- [9] C. Zhu *et al.*, "Statistical moments-based OSNR monitoring for coherent optical systems," *Opt. Exp.*, vol. 20, no. 16, pp. 17711–17721, 2012.
- [10] J. Yuan *et al.*, "OSNR monitoring in presence of fiber nonlinearities for coherent Nyquist-WDM system," *Opt. Commun.*, vol. 380, pp. 10–14, 2016.
- [11] E. Ip and J. M. Kahn, "Compensation of dispersion and nonlinear impairments using digital backpropagation," *IEEE J. Lightw. Technol.*, vol. 208, no. 26, pp. 3416–3425, Oct. 2008.
- [12] A. Mecozzi, C. B. Clausen, and M. Shtaif, "Analysis of intrachannel nonlinear effects in highly dispersed optical pulse transmission," *IEEE Photon. Technol. Lett.*, vol. 12, no. 4, pp. 392–394, Apr. 2000.
- [13] K. V. Peddanarappagari and M. Brandt-Pearce, "Volterra series transfer function of single-mode fibers," *IEEE J. Lightw. Technol.*, vol. 15, no. 12, pp. 2232–2241, Dec. 1997.
- [14] J. Tang, "The channel capacity of a multispan DWDM system employing dispersive nonlinear optical fibers and an ideal coherent optical receiver," *IEEE J. Lightw. Technol.*, vol. 20, no. 7, pp. 1095–1101, Jul. 2002.
- [15] A. Carena, V. Curri, G. Bosco, P. Poggiolini, and F. Forghieri, "Modeling of the impact of nonlinear propagation effects in uncompensated optical coherent transmission links," *IEEE J. Lightw. Technol.*, vol. 30, no. 10, pp. 1524–1539, May 2012.
- [16] G. P. Agrawal, *Fiber Optic Communication Systems*, 4th ed. New York, NY, USA: Wiley, 2010.
- [17] G. P. Agrawal, *Nonlinear Fiber Optics*, 4th ed. New York, NY, USA: Elsevier, 2009.
- [18] C. C. K. Chan, *Optical Performance Monitoring: Advanced Techniques for Next-Generation Photonic Networks*, 1st ed. San Diego, CA, USA: Elsevier, 2010.
- [19] S. P. Singh and N. Singh, "Nonlinear effects in optical fibers: Origin, management and applications," *Progress Electromagn. Res.*, vol. 73, pp. 249–275, 2007.